Nano Research
2020, 13(5): 1479–1484
ISSN 1998-0124 CN 11-5974/O4
https://doi.org/10.1007/s12274-020-2825-6

Research Article

Bioelectronic protein nanowire sensors for ammonia detection

Alexander F. Smith[1], Xiaomeng Liu[2], Trevor L. Woodard[3], Tianda Fu[2], Todd Emrick[4], Juan M. Jiménez[1,5,6], Derek R. Lovley[3,6] (✉), and Jun Yao[1,2,6] (✉)

[1] *Department of Biomedical Engineering, University of Massachusetts, Amherst, MA 01003, USA*
[2] *Department of Electrical and Computer Engineering, University of Massachusetts, Amherst, MA 01003, USA*
[3] *Department of Microbiology, University of Massachusetts, Amherst, MA 01003, USA*
[4] *Department of Polymer Science and Engineering, University of Massachusetts, Amherst, MA 01003, USA*
[5] *Department of Mechanical and Industrial Engineering, University of Massachusetts, Amherst, MA 01003, USA*
[6] *Institute for Applied Life Sciences (IALS), University of Massachusetts, Amherst, MA 01003, USA*

Received: 20 February 2020 / **Revised:** 7 April 2020 / **Accepted:** 19 April 2020

ABSTRACT

Electronic sensors based on biomaterials can lead to novel green technologies that are low cost, renewable, and eco-friendly. Here we demonstrate bioelectronic ammonia sensors made from protein nanowires harvested from the microorganism *Geobacter sulfurreducens*. The nanowire sensor responds to a broad range of ammonia concentrations (10 to 10^6 ppb), which covers the range relevant for industrial, environmental, and biomedical applications. The sensor also demonstrates high selectivity to ammonia compared to moisture and other common gases found in human breath. These results provide a proof-of-concept demonstration for developing protein nanowire based gas sensors for applications in industry, agriculture, environmental monitoring, and healthcare.

KEYWORDS

nanowire, protein nanowire, biomaterial, bioelectronics, biosensor, ammonia sensor

1 Introduction

Methods to quantify the constituents of gases have important applications in industry, agriculture, environmental monitoring, and healthcare. Ammonia is often a key gaseous component [1]. For example, ammonia is commonly used to produce fertilizers and pharmaceuticals, but can be toxic if inhaled [1]. In poultry farming, the ammonia levels need to be closely monitored and controlled as high levels lead to production losses, higher feed conversion ratios, compromised bird health, and non-compliance with animal welfare guidelines [2]. Environmental monitoring of ammonia is important because its toxicity has damaging effects on the ecosystem and human health [3–5]. Accurate environmental monitoring of ammonia gas concentrations near cities requires sensitivity in the 20–30 ppb range [4]. For potential biomedical applications, high levels of ammonia in the breath may indicate asthma and bacterial infections in the lungs [6, 7], as well as chronic kidney disease (CKD). Healthy human ammonia breath concentrations are usually sub-ppm (< 1 ppm), ranging from ~ 30 to 1,800 ppb [7–13], but are typically elevated to multiple ppm (~ 1–15 or a mean ~ 5 ppm) [8] in the case of renal damage and CKD [7, 8, 10, 13]. This effect is not exclusive to adult patients, since elevated levels of breath ammonia have also been observed in the earliest stages of pediatric CKD patients [14]. Renal and liver diseases can be tracked with ammonia breath levels [7, 8, 15, 16], which are also useful for monitoring halitosis [7, 17] and epileptic patients [7]. Altogether, there is clearly a need to evaluate patients by measuring ammonia in the breath using portable point-of-care sensors.

Electronic biosensors are advantageous due to their compact size and easy integration, enabling portable point-of-care diagnostics [18]. Various electronic sensors based on carbon nanotubes [19–25], silicon nanowires [26–29], metal oxides [24, 30–36], and other hybrid materials [37–42] have been developed for ammonia detection, but the majority lack the sub-ppm sensitivity required for environmental and health monitoring. Incorporating low-dimensional nanomaterials for improved surface coupling and signal transduction has, in some instances, enabled ammonia detection at tens of ppb [4, 43, 44] based on conductance modulation through field or charge effects introduced by ammonia adsorption. However, the selectivity of these sensors for ammonia and their susceptibility to nonspecific interference is not well known, as surface adsorbates can have generic charge or field effects that modulate the conductance in nanomaterials [45]. Ammonia sensors based on optical waveguide techniques typically incorporate pH sensing dyes that are responsive to adsorbed ammonia [46]. Optical waveguide sensors can achieve high sensitivity for ammonia detection [46], but are often too large, complex, and expensive for portable applications.

Electrically conductive protein nanowires are a potential alternative active component of electronic sensors [47, 48]. Protein nanowires were shown to be highly responsive to pH with a widely tunable conductivity, indicating the effect of proton doping [49, 50]. Since ammonia is known to modulate protonation, protein nanowires may be a promising candidate for highly sensitive and selective ammonia sensing. In addition, protein nanowires can be microbially produced from renewable

Address correspondence to Derek R. Lovley, dlovley@microbio.umass.edu; Jun Yao, juny@umass.edu

feedstocks at a fraction of the energy requirements for fabricating silicon nanowires or carbon nanotubes, without harsh chemical processes or toxic components in the final product [47, 48]. Although they are physically and chemically robust (functional at pH 2–10.5 and temperatures up to ca. 100 °C) [47, 48, 50], protein nanowires are biodegradable, eliminating the growing environmental and health concerns associated with electronic waste [48, 51, 52]. Thus, protein nanowires are an attractive sustainable, "green" electronic material.

Here we demonstrate that highly effective electronic ammonia gas sensors can be made from protein nanowires harvested from the microorganism *Geobacter sulfurreducens*. The sensors detected ammonia at low (10 ppb) concentrations with high selectivity among various gases commonly found in breath, indicating the potential for disease monitoring in biomedical applications.

2 Experimental section

2.1 Fabrication of protein nanowire sensors

Protein nanowires (Fig. 1(a)) were purified from cultures of *Geobacter sulfurreducens* as previously described [53], and suspended in water. Interdigitated electrodes were fabricated on polyethylene terephthalate (PET) substates with standard lithography, metal deposition (Cr/Au, 3/50 nm), and lift-off processes. Scotch tape was used to define a 10 mm × 2 mm area to be deposited with the protein nanowire film. The prepared protein nanowire solution was drop-casted across the Au electrodes on the substrate, and the water in the protein nanowire solution was dried at 23 °C, to fabricate the thin-film sensor structure (Figs. 1(b) and 1(c)). Film thickness was estimated using an optical profilometer.

2.2 Electrical measurement setup

The protein nanowire sensor was placed in a custom-built airtight vapor chamber to control gas concentration (Fig. S1 in the Electronic Supplementary Material (ESM)). A gas injection port was designed to inject ammonia gas via syringe into the chamber. A miniature fan was installed within the vapor chamber to disperse the gas throughout the chamber. The baseline humidity in the chamber was controlled by tuning the equilibrium vapor pressure of sulfuric acid solutions by varying the concentration of sulfuric acid [54]. The humidity was measured continuously using a hygrometer (Reed 6030). Temperature was kept constant at 23 °C.

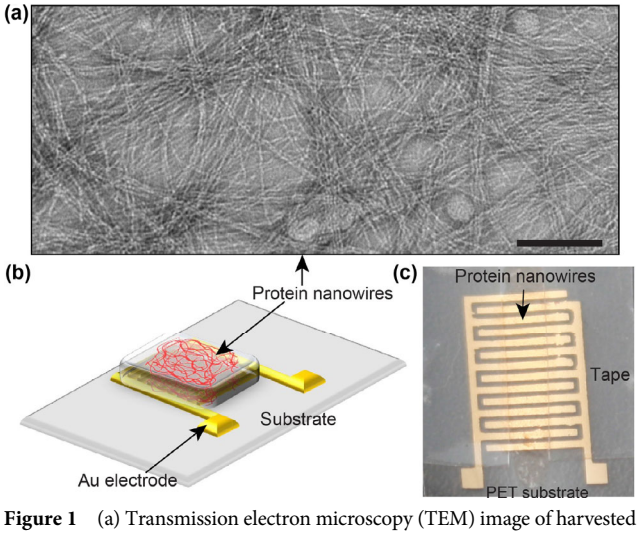

Figure 1 (a) Transmission electron microscopy (TEM) image of harvested protein nanowires for sensor devices. Scale bar, 100 nm. (b) Schematic of the sensor device made by drop-casting protein nanowires on gold electrodes. (c) Photograph of a protein nanowire sensor fabricated on a PET substrate; scotch tape defined the assembly region.

During electrical measurements, a constant voltage of 1 V was applied to the sensor and the current was measured continuously by a semiconductor parameter analyzer (Keithley 4200-SCS). The vapor chamber was sealed to maintain a constant relative humidity level. A syringe was used to extract volatilized gas from the head space of a container of ammonium hydroxide (32%, Merck) *in-situ* and inject the gas directly into the vapor chamber through the gas injection port. The concentration of the injected ammonia gas was calculated using the ideal gas law, given the known partial pressure of ammonia in the ammonium hydroxide solution. After the sensor response reached a steady state signal, ammonia gas was purged from the vapor chamber, returning the current output to its original state.

To test the humidity response of the sensor, the relative humidity was varied from 45%–100% by evaporating a droplet of water inside the vapor chamber. The current output was continuously measured, as was the humidity level using the hygrometer. To analyze the isolated effect of water vapor (e.g., compared to a mixture of ammonia and water vapor), pure water vapor was injected via the syringe.

To elucidate the response of protein nanowire sensor to various gases, the syringe injection method was used to expose the sensor to gases and volatile organic compounds (VOCs) that are commonly found in the breath. Physiological concentrations of 1 ppm ammonia, acetone, and ethanol gases were tested by injecting gas extracted from the headspace of containers of liquid. Nitrogen and carbon dioxide were directly injected as pure gases.

3 Results and discussion

The sensors were made by depositing a protein nanowire suspension on interdigitated electrodes to yield a thin conductive film after air-drying (Figs. 1(b) and 1(c)). It was previously shown that a thicker protein nanowire film yielded a lower adsorption of gas molecules (e.g., moisture) due to an increasing diffusion barrier to deeper layers [55]. As a result, we expect reduced gas sensitivity in thicker protein nanowire films, a trend that is also observed in other nanomaterials [56, 57]. This may result from a reduced effective surface-to-volume ratio in thicker films. Therefore, we used a thin layer of protein nanowires (e.g., ~ 40 nm with $\sigma = 2.3 \times 10^{-7}$ S/cm) for testing with potentially improved sensitivity. The nanowire sensor was biased at a constant direct current (DC) voltage of 1 V, and current was monitored in real-time as dilute ammonia gas was repeatedly injected into and purged from the vapor testing chamber (Fig. S1 in the ESM). Increasing the concentration of ammonia gas introduced to the chamber yielded a distinct increase in current (Fig. 2(a)). The sensor responded to a broad range of ammonia concentrations (Fig. 2(b)), with a lower detection limit of 10 ppb. This is, to our knowledge, among the lowest detection limits of existing electronic ammonia sensors [4, 43, 44] (Table 1). Sensor sensitivity, defined as the relative conductance change ($\Delta G/G$) per ppm, increased at lower concentrations (Fig. 2(b)), which is commonly observed in other ammonia sensors [20, 21, 23, 28, 38, 41, 58]. The dynamic response range of the sensor is suitable for most environmental and biomedical applications (e.g., 30–15,000 ppb) [8, 9, 13]. The response time of the sensor, defined as the time required for the baseline current signal to increase to 90% of its peak saturation value, was 46 s, which is faster than most existing electronic ammonia gas sensors that can achieve low (e.g., sub-ppm) detection (Table 1). Repeated exposures to

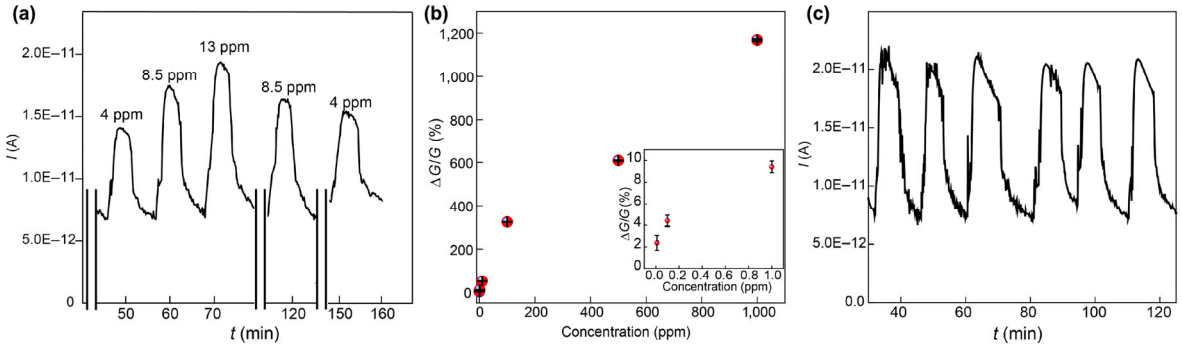

Figure 2 (a) Real-time response of the nanowire sensor to injected ammonia gas at a baseline relative humidity of 45%. (b) Sensor response ($\Delta G/G$ %) with respect to a wide range of ammonia concentrations (10 ppb to 1,000 ppm) at 55 %RH. The inset shows the response from 10 ppb to 1 ppm. (c) Reproducible responses from the sensor by repeated injection of 8.5 ppm ammonia at 50 %RH. The temperature was kept constant at 23 °C.

Table 1 Comparison of protein nanowire sensor with representative electronic ammonia gas sensors

Material	Sensitivity range (ppb)	Measured limit of detection (ppb)	Response time (s)	Reference
Protein nanowires (this work)	10–1,000,000	10	46	This work
SWCNT/indium-tin oxide (ITO) nanoparticles	20–3,400,000	20	~ 60; not reported	[4, 43]
SWCNT/COOH-functionalization	30–30,000	30	60	[25]
Si NW/SiO_2	170–20,000	170	900	[29]
Si NW/tellurium nanoparticles	10,000–400,000	10,000	5	[28]
MoO_3	50–1,000	50	not reported	[44]
Perovskite halide ($CH_3NH_3PbI_3$)	1,000–50,000	1,000	~ 100–130	[41]
rGO/Co_3O_4 nanofibers	5,000–100,000	5,000	4	[40]

8.5 ppm ammonia gas demonstrated that the electrical response was consistent and reproducible (Fig. 2(c)). As protein nanowires are highly stable in ambient environments, the protein nanowire sensors demonstrated robust functionality, maintaining a consistent response when tested repeatedly over 90 days (Fig. S2 in the ESM). The result is consistent with a previous study demonstrating long-term stability of a protein nanowire device in an ambient environment [55], which can be attributed to the material robustness in protein nanowires even in harsh environments [47, 48, 50].

Water can affect the sensing signals of various electronic ammonia sensors [4, 43, 44, 58–61]. Therefore, the conductance of the protein nanowire sensor was measured over a range of relative humidity, from 45%–100%. It was observed that the conductance changed by approximately three orders of magnitude (Fig. S3(a) in the ESM). Low-dimension electronic materials are often highly responsive to humidity [4, 43, 44, 61]. Proton conduction assisted by adsorbed water molecules may account for this conductance increase [61]. The protein nanowires adsorb considerable moisture [55] (Fig. S4 in the ESM), due to a high density of hygroscopic functional groups in the constituent amino acids (e.g., carboxyl and amine groups) [62, 63].

The protein nanowire sensor exhibited a much stronger response to ammonia than to moisture. The maximal sensitivity to water vapor, extrapolated from the current response curve, was ~ 0.25% ppm^{-1} with an average < 0.1% ppm^{-1} (Fig. S3(b) in the ESM), whereas the sensitivity to ammonia was 9.4% ppm^{-1} at low concentrations and an average > 1% ppm^{-1} over the full range of ammonia concentrations evaluated (Fig. 2(b)). Additional analysis demonstrated that the sensor response to water vapor was negligible compared to the response to ammonia gas (Fig. 3(a)).

In order to further evaluate the influence of humidity on ammonia sensing, the ambient humidity inside the vapor chamber was varied (35%–90%) to study the electrical response of the sensor at different initial baseline conductivities after injecting ammonia concentrations of 10 ppm. There was no substantial difference in response to ammonia over this broad range of humidity (Fig. 3(b)). This converged ammonia sensitivity (e.g., > 4% ppm^{-1}) indicated that the sensor functions effectively

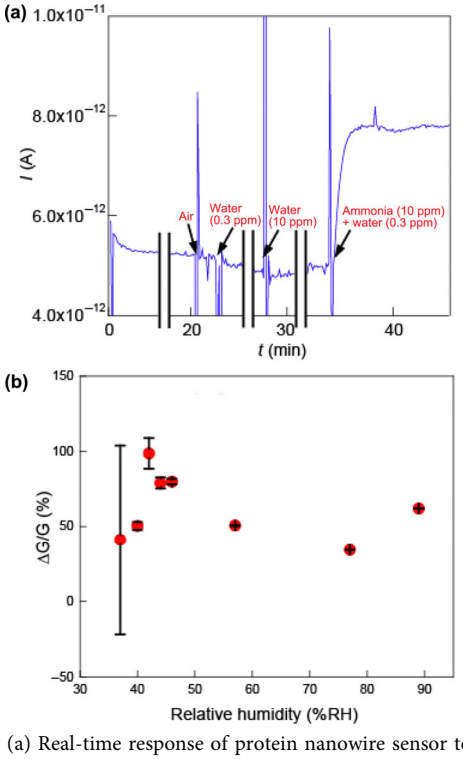

Figure 3 (a) Real-time response of protein nanowire sensor to injected air, pure water vapor (0.3 and 10 ppm), and a mixture containing 10 ppm ammonia + 0.3 ppm water vapor. The initial sharp spike for each injection results from an artifact (e.g., mechanical perturbation to contacts/connections). Temperature was kept constant at 23 °C. (b) Dose-dependent response of protein nanowire sensors to injected ammonia gas (10 ppm) at various baseline environmental relative humidity levels.

in varied environmental humidity, maintaining excellent sensing performance.

Analysis of ammonia in breath for disease diagnosis requires the ability to discriminate between ammonia and other common breath components. At a concentration of 1 ppm, ammonia gas elicited a percent change in current of 10.3%, significantly higher than the response to acetone, ethanol, carbon dioxide, or nitrogen, with percent changes of 0.13%, 0.33%, 0.23%, and −0.02%, respectively (Fig. 4).

The results demonstrate that protein nanowires can function as highly sensitive, selective, and robust sensors for ammonia with ultra-low power consumption (e.g., ~ picowatt (pW), Fig. 3(a)). The unique structural and physical/chemical properties of protein nanowires may account for the changes in the protein nanowire thin-film conductivity in the presence of ammonia. Specifically, protein nanowire films contain abundant nanometer or subnanometer pores at the nanowire-nanowire interfaces [55], providing more opportunities for ammonia gas permeation into the films and more gas-nanowire surface interactions than in existing thin-film sensors [31, 58, 59, 64, 65]. Meanwhile, a high density of hygroscopic groups (e.g., amine and carboxyl groups with an estimated density of 10 nm^{-1}) innate to protein nanowires [55, 62] may promote the adsorption of water and ammonia through hydrogen bonding. The small diameter of protein nanowires (e.g., 3 nm) results in a large effective surface area for adsorption. As a result, a substantial adsorption of moisture from the ambient atmosphere was experimentally observed [55]. Surface water adsorption in turn can further enhance ammonia adsorption [66]. Collectively, the protein nanowire film is expected to be highly effective in ammonia adsorption.

Previous studies of *Geobacter* protein nanowires showed that a low pH in the preparation solution could substantially enhance the conductivity in individual nanowires or nanowire thin films [49]. It was also indicated that a wild-type nanowire film had a p-type conduction trend [67]. These findings suggested the possibility that proton-doping mediates the conductance modulation in protein nanowires. We speculate that ionization in adsorbed ammonia, which was revealed to be greatly enhanced with a molecular layer of water [68], produces protonation sites (e.g., NH_4^+) that yield similar doping effects to the protein nanowires. However, the conduction mechanisms in *Geobacter* protein nanowires are not fully understood [47], which makes it difficult to develop an in-depth mechanistic understanding for how the doping effect from ammonia modifies protein nanowire film conductivity. In addition, proton transport through the Grotthuass mechanism [69] ($NH_4^+ + NH_3 \rightarrow NH_3 + NH_4^+$) may further contribute to the increased conductance. The recent development of a method for producing electrically conductive protein nanowires with *Escherichia coli* can now provide the substantial quantities of protein nanowires required for further mechanistic studies [70].

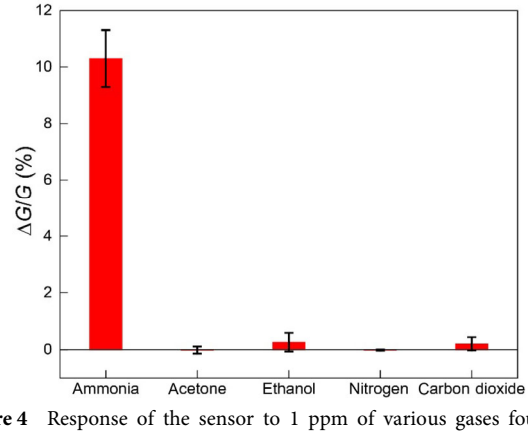

Figure 4 Response of the sensor to 1 ppm of various gases found in human breath using the syringe injection method. Temperature was kept constant at 23 °C.

In addition, a protein nanowire sensor integrated on a 25 μm-thick polyimide (PI) substrate can be folded (e.g., at a bending radius < 1 mm), demonstrating a negligible change in conductance (Fig. S5(a) in the ESM). As a result, the sensor attached to a finger joint experienced minimal mechanical perturbation during bending (Fig. S5(b) in the ESM). These preliminary results provide evidence that the protein nanowire sensors can sustain mechanical strain induced from body movements for flexible and wearable applications [71].

4 Conclusions

In conclusion, we have demonstrated a novel type of electronic ammonia sensor made from sustainably produced protein nanowires. The high sensitivity and selectivity demonstrated here indicate the potential for ammonia sensing in healthcare and environmental applications. The outer surface of protein nanowires can be further decorated with peptide ligands [72] designed to specifically bind chemicals of interest, suggesting possibilities to develop sensors for the detection of a wide range of analytes. These capabilities, coupled with the sustainable fabrication and disposal properties of protein nanowires [48], suggest that protein nanowires will prove to be desirable sensing components for applications in industry, agriculture, environmental monitoring, and healthcare.

Acknowledgements

J. Y. and D. R. L. acknowledge support from a seed fund through the Office of Technology Commercialization and Ventures at the University of Massachusetts, Amherst. J. Y. acknowledges the support from a National Science Foundation (NSF) Award ECCS-1917630. J. M. J. acknowledges support from a NSF grants CAREER CMMI1842308. A. F. S. acknowledges the support from a NSF Graduate Research Fellowship (No. S12100000000937). Part of the device fabrication work was conducted in the clean room of the Center for Hierarchical Manufacturing (CHM), an NSF Nanoscale Science and Engineering Center (NSEC) located at the University of Massachusetts, Amherst.

Electronic Supplementary Material: Supplementary material (experimental setup, device stability, humidity response, and moisture content) is available in the online version of this article at https://doi.org/10.1007/s12274-020-2825-6.

References

[1] Kwak, D.; Lei, Y.; Maric, R. Ammonia gas sensors: A comprehensive review. *Talanta* **2019**, *204*, 713–720.

[2] Ritz, C. W.; Fairchild, B. D.; Lacy, M. P. Implications of ammonia production and emissions from commercial poultry facilities: A review. *J. Appl. Poult. Res.* **2004**, *13*, 684–692.

[3] van der Eerden, L. J. M.; de Visser, P. H. B.; van Dijk, C. J. Risk of damage to crops in the direct neighbourhood of ammonia sources. *Environ. Pollut.* **1998**, *102*, 49–53.

[4] Rigoni, F.; Tognolini, S.; Borghetti, P.; Drera, G.; Pagliara, S.; Goldoni, A.; Sangaletti, L. Environmental monitoring of low-ppb ammonia concentrations based on single-wall carbon nanotube chemiresistor gas sensors: Detection limits, response dynamics, and moisture effects. *Procedia Eng.* **2014**, *87*, 716–719.

[5] Baek, B. H.; Aneja, V. P.; Tong, Q. S. Chemical coupling between ammonia, acid gases, and fine particles. *Environ. Pollut.* **2004**, *129*, 89–98.

[6] Kharitonov, S. A.; Barnes, P. J. Biomarkers of some pulmonary diseases in exhaled breath. *Biomarkers* **2002**, *7*, 1–32.
[7] Bayrakli, I.; Turkmen, A.; Akman, H.; Sezer, M. T.; Kutluhan, S. Applications of external cavity diode laser-based technique to noninvasive clinical diagnosis using expired breath ammonia analysis: Chronic kidney disease, epilepsy. *J. Biomed. Opt.* **2016**, *21*, 87004.
[8] Davies, S.; Spanel, P.; Smith, D. Quantitative analysis of ammonia on the breath of patients in end-stage renal failure. *Kidney Int.* **1997**, *52*, 223–228.
[9] Hibbard, T.; Killard, A. J. Breath ammonia levels in a normal human population study as determined by photoacoustic laser spectroscopy. *J. Breath Res.* **2011**, *5*, 037101.
[10] Bevc, S.; Mohorko, E.; Kolar, M.; Brglez, P.; Holobar, A.; Kniepeiss, D.; Podbregar, M.; Piko, N.; Hojs, N.; Knehtl, M. et al. Measurement of breath ammonia for detection of patients with chronic kidney disease. *Clin. Nephrol.* **2017**, *88*, 14–17.
[11] Turner, C.; Španěl, P.; Smith, D. A longitudinal study of ammonia, acetone and propanol in the exhaled breath of 30 subjects using selected ion flow tube mass spectrometry, SIFT-MS. *Physiol. Meas.* **2006**, *27*, 321–337.
[12] Mathew, T. L.; Pownraj, P.; Abdulla, S.; Pullithadathil, B. Technologies for clinical diagnosis using expired human breath analysis. *Diagnostics* **2015**, *5*, 27–60.
[13] Güntner, A. T.; Righettoni, M.; Pratsinis, S. E. Selective sensing of NH_3 by Si-doped-MoO_3 for breath analysis. *Sens. Actuators B: Chem.* **2016**, *223*, 266–273.
[14] Obermeier, J.; Trefz, P.; Happ, J.; Schubert, J. K.; Staude, H.; Fischer, D. C.; Miekisch, W. Exhaled volatile substances mirror clinical conditions in pediatric chronic kidney disease. *PLoS One* **2017**, *12*, e0178745.
[15] Sawicka, K.; Gouma, P.; Simon, S. Electrospun biocomposite nanofibers for urea biosensing. *Sens. Actuators B: Chem.* **2005**, *108*, 585–588.
[16] Narasimhan, L. R.; Goodman, W.; Patel, C. K. N. Correlation of breath ammonia with blood urea nitrogen and creatinine during hemodialysis. *Proc. Natl. Acad. Sci. USA* **2001**, *98*, 4617–4621.
[17] Amano, A.; Yoshida, Y.; Oho, T.; Koga, T. Monitoring ammonia to assess halitosis. *Oral Surg. Oral Med. Oral Pathol. Oral Radiol. Endod.* **2002**, *94*, 692–696.
[18] Turner, A. P. F. Biosensors: Sense and sensibility. *Chem. Soc. Rev* **2013**, *42*, 3184–3196.
[19] Piloto, C.; Mirri, F.; Bengio, E. A.; Notarianni, M.; Gupta, B.; Shafiei, M.; Pasquali, M.; Motta, N. Room temperature gas sensing properties of ultrathin carbon nanotube films by surfactant-free dip coating. *Sens. Actuators B: Chem.* **2016**, *227*, 128–134.
[20] Bekyarova, E.; Davis, M.; Burch, T.; Itkis, M. E.; Zhao, B.; Sunshine, S.; Haddon, R. C. Chemically functionalized single-walled carbon nanotubes as ammonia sensors. *J. Phys. Chem. B.* **2004**, *108*, 19717–19720.
[21] Chopra, S.; Pham, A.; Gaillard, J.; Parker, A.; Rao, A. M. Carbon-nanotube-based resonant-circuit sensor for ammonia. *Appl. Phys. Lett.* **2002**, *80*, 4632–4634.
[22] Quang, N. H.; Van Trinh, M.; Lee, B. H.; Huh, J. S. Effect of NH_3 gas on the electrical properties of single-walled carbon nanotube bundles. *Sens. Actuators B: Chem.* **2006**, *113*, 341–346.
[23] Van Hieu, N.; Dung, N. Q.; Tam, P. D.; Trung, T.; Chien, N. D. Thin film polypyrrole/SWCNTs nanocomposites-based NH_3 sensor operated at room temperature. *Sens. Actuators B: Chem.* **2009**, *140*, 500–507.
[24] Duc Hoa, N.; Van Quy, N.; Suk Cho, Y.; Kim, D. Nanocomposite of SWNTs and SnO_2 fabricated by soldering process for ammonia gas sensor application. *Phys. Status Solidi* **2007**, *204*, 1820–1824.
[25] Rigoni, F.; Freddi, S.; Pagliara, S.; Drera, G.; Sangaletti, L.; Suisse, J. M.; Bouvet, M.; Malovichko, A. M.; Emelianov, A. V.; Bobrinetskiy, I. I. Humidity-enhanced sub-ppm sensitivity to ammonia of covalently functionalized single-wall carbon nanotube bundle layers. *Nnano-technology* **2017**, *28*, 255502.
[26] Fobelets, K.; Panteli, C.; Sydoruk, O.; Li, C. B. Ammonia sensing using arrays of silicon nanowires and graphene. *J. Semicond.* **2018**, *39*, 063001.
[27] In, H. J.; Field, C. R.; Pehrsson, P. E. Periodically porous top electrodes on vertical nanowire arrays for highly sensitive gas detection. *Nanotechnology* **2011**, *22*, 355501.
[28] Yang, L.; Lin, H. Y.; Zhang, Z. S.; Cheng, L.; Ye, S. Y.; Shao, M. W. Gas sensing of tellurium-modified silicon nanowires to ammonia and propylamine. *Sens. Actuators B: Chem.* **2013**, *177*, 260–264.
[29] Schmädicke, C. Silicon nanowire based sensor for highly sensitive and selective detection of ammonia. Ph.D. Dissertation, The Technische Universität Dresden, Dresden, Germany, 2015.
[30] Betty, C. A.; Choudhury, S.; Girija, K. G. Discerning specific gas sensing at room temperature by ultrathin SnO_2 films using impedance approach. *Sens. Actuators B: Chem.* **2012**, *173*, 781–788.
[31] Van Hieu, N.; Thuy, L. T. B.; Chien, N. D. Highly sensitive thin film NH_3 gas sensor operating at room temperature based on SnO_2/MWCNTs composite. *Sens. Actuators B: Chem.* **2008**, *129*, 888–895.
[32] Kumar, L.; Rawal, I.; Kaur, A.; Annapoorni, S. Flexible room temperature ammonia sensor based on polyaniline. *Sens. Actuators B: Chem.* **2017**, *240*, 408–416.
[33] Van Tuan, C.; Tuan, M. A.; Van Hieu, N.; Trung, T. Electrochemical synthesis of polyaniline nanowires on Pt interdigitated microelectrode for room temperature NH_3 gas sensor application. *Curr. Appl. Phys.* **2012**, *12*, 1011–1016.
[34] Deshpande, N. G.; Gudage, Y. G; Sharma, R.; Vyas, J. C.; Kim, J. B.; Lee, Y. P. Studies on tin oxide-intercalated polyaniline nanocomposite for ammonia gas sensing applications. *Sens. Actuators B: Chem.* **2009**, *138*, 76–84.
[35] Tran, Q. T.; Hoa, H. T. M.; Yoo, D. H.; Cuong, T. V.; Hur, S. H.; Chung, J. S.; Kim, E. J.; Klohl, P. A. Reduced graphene oxide as an over-coating layer on silver nanostructures for detecting NH_3 gas at room temperature. *Sens. Actuators B: Chem.* **2014**, *194*, 45–50.
[36] Biskupski, D.; Herbig, B.; Schottner, G.; Moos, R. Nanosized titania derived from a novel sol–gel process for ammonia gas sensor applications. *Sens. Actuators B: Chem.* **2011**, *153*, 329–334.
[37] Andre, R. S.; Kwak, D.; Dong, Q. C.; Zhong, W.; Correa, D. S.; Mattoso, L. H. C.; Lei, Y. Sensitive and selective NH_3 monitoring at room temperature using ZnO ceramic nanofibers decorated with poly(styrene sulfonate). *Sensors (Basel)* **2018**, *18*, 1058.
[38] Pang, Z. Y.; Yang, Z. P.; Chen, Y.; Zhang, J. N.; Wang, Q. Q.; Huang, F. L.; Wei, Q. F. A room temperature ammonia gas sensor based on cellulose/TiO_2/PANI composite nanofibers. *Colloids Surf. A: Physicochem. Eng. Asp.* **2016**, *494*, 248–255.
[39] Lin, Q. Q.; Li, Y.; Yang, M. J. Tin oxide/graphene composite fabricated via a hydrothermal method for gas sensors working at room temperature. *Sens. Actuators B: Chem.* **2012**, *173*, 139–147.
[40] Feng, Q. X.; Li, X. G.; Wang, J.; Gaskov, A. M. Reduced graphene oxide (rGO) encapsulated Co_3O_4 composite nanofibers for highly selective ammonia sensors. *Sens. Actuators B: Chem.* **2016**, *222*, 864–870.
[41] Maity, A.; Raychaudhuri, A. K.; Ghosh, B. High sensitivity NH_3 gas sensor with electrical readout made on paper with perovskite halide as sensor material. *Sci. Rep.* **2019**, *9*, 7777.
[42] Aba, L.; Yusuf, Y.; Mitrayana; Siswanta, D.; Junaidi; Triyana, K. Sensitivity improvement of ammonia gas sensor based on poly(3,4-ethylenedioxythiophene): Poly(styrenesulfonate) by employing doping of bromocresol green. *J. Nanotechnol.* **2014**, *2014*, 864274.
[43] Rigoni, F.; Drera, G.; Pagliara, S.; Goldoni, A.; Sangaletti, L. High sensitivity, moisture selective, ammonia gas sensors based on single-walled carbon nanotubes functionalized with indium tin oxide nanoparticles. *Carbon* **2014**, *80*, 356–363.
[44] Gouma, P.; Kalyanasundaram, K.; Yun, X.; Stanacevic, M.; Wang, L. S. Nanosensor and breath analyzer for ammonia detection in exhaled human breath. *IEEE Sens. J.* **2010**, *10*, 49–53.
[45] Yao, J.; Jin, Z.; Zhong, L.; Natelson, D.; Tour, J. M. Two-terminal nonvolatile memories based on single-walled carbon nanotubes. *ACS Nano* **2009**, *3*, 4122–4126.
[46] Yimit, A.; Itoh, K.; Murabayashi, M. Detection of ammonia in the ppt range based on a composite optical waveguide pH sensor. *Sens. Actuators B: Chem.* **2003**, *88*, 239–245.
[47] Lovley, D. R. Electrically conductive pili: Biological function and potential applications in electronics. *Curr. Opin. Electrochem.* **2017**, *4*, 190–198.
[48] Lovley, D. R. e-Biologics: Fabrication of sustainable electronics with "green" biological materials. *mBio* **2017**, *8*, e00695-17.
[49] Adhikari, R. Y.; Malvankar, N. S.; Tuominen, M. T.; Lovley, D. R. Conductivity of individual *Geobacter* pili. *RSC Adv.* **2016**, *6*, 8354–8357.

[50] Sun, Y. L.; Tang, H. Y.; Ribbe, A.; Duzhko, V.; Woodard, T. L.; Ward, J. E.; Bai, Y.; Nevin, K. P.; Nonnenmann, S. S.; Russell, T. et al. Conductive composite materials fabricated from microbially produced protein nanowires. *Small* **2018**, *14*, 1802624.
[51] Kumar, A.; Holuszko, M.; Espinosa, D. C. R. E-waste: An overview on generation, collection, legislation and recycling practices. *Resour. Conserv. Recycl.* **2017**, *122*, 32–42.
[52] Tansel, B. From electronic consumer products to e-wastes: Global outlook, waste quantities, recycling challenges. *Environ. Int.* **2017**, *98*, 35–45.
[53] Tan, Y.; Adhikari, R. Y.; Malvankar, N. S.; Ward, J. E.; Woodard, T. L.; Nevin, K. P.; Lovley, D. R. Expressing the *Geobacter metallireducens* PilA in *Geobacter sulfurreducens* yields pili with exceptional conductivity. *mBio* **2017**, *8*, e02203-16.
[54] Feng, J.; Peng, L. L.; Wu, C. Z.; Sun, X.; Hu, S. L.; Lin, C. W.; Dai, J.; Yang, J. L.; Xie, Y. Giant moisture responsiveness of VS_2 ultrathin nanosheets for novel touchless positioning interface. *Adv. Mater.* **2012**, *24*, 1969–1974.
[55] Liu, X. M.; Gao, H. Y.; Ward, J. E.; Liu, X. R.; Yin, B.; Fu, T. D.; Chen, J. H.; Lovley, D. R.; Yao, J. Power generation from ambient humidity using protein nanowires. *Nature* **2020**, *578*, 550–554.
[56] Cui, S. M.; Pu, H. H.; Wells, S. A.; Wen, Z. H.; Mao, S.; Chang, J. B.; Hersam, M. C.; Chen, C. H. Ultrahigh sensitivity and layer-dependent sensing performance of phosphorene-based gas sensors. *Nat. Commun.* **2015**, *6*, 8632.
[57] Donarelli, M.; Ottaviano, L. 2D materials for gas sensing applications: A review on graphene oxide, MoS_2, WS_2 and phosphorene. *Sensors* **2018**, *18*, 3638.
[58] Jian, J. M.; Guo, X. S.; Lin, L. W.; Cai, Q.; Cheng, J.; Li, J. P. Gas-sensing characteristics of dielectrophoretically assembled composite film of oxygen plasma-treated SWCNTs and PEDOT/PSS polymer. *Sens. Actuators B: Chem.* **2013**, *178*, 279–288.
[59] Pandey, S.; Nanda, K. K. Au nanocomposite based chemiresistive ammonia sensor for health monitoring. *ACS Sensors* **2016**, *1*, 55–62.
[60] Suri, K.; Annapoorni, S.; Sarkar, A. K.; Tandon, R. P. Gas and humidity sensors based on iron oxide-polypyrrole nanocomposites. *Sens. Actuators B: Chem.* **2002**, *81*, 277–282.
[61] Bi, H. C.; Yin, K. B.; Xie, X.; Ji, J.; Wan, S.; Sun, L. T.; Terrones, M.; Dresselhaus, M. S. Ultrahigh humidity sensitivity of graphene oxide. *Sci. Rep.* **2013**, *3*, 2714.
[62] Xiao, K.; Malvankar, N. S.; Shu, C. J.; Martz, E.; Lovley, D. R.; Sun, X. Low energy atomic models suggesting a pilus structure that could account for electrical conductivity of *Geobacter sulfurreducens* pili. *Sci. Rep.* **2016**, *6*, 23385.
[63] Feliciano, G. T.; Steidl, R. J.; Reguera, G. Structural and functional insights into the conductive pili of *Geobacter sulfurreducens* revealed in molecular dynamics simulations. *Phys. Chem. Chem. Phys.* **2015**, *17*, 22217–22226.
[64] Philip, B.; Abraham, J. K.; Chandrasekhar, A.; Varadan, V. K. Carbon nanotube/PMMA composite thin films for gas-sensing applications. *Smart Mater. Struct.* **2003**, *12*, 935–939.
[65] Li, C.; Zhang, D. H.; Liu, X. L.; Han, S.; Tang, T.; Han, J.; Zhou, C. W. In_2O_3 nanowires as chemical sensors. *Appl. Phys. Lett.* **20013**, *82*, 1613.
[66] Tang, S. B.; Cao, Z. X. Adsorption and dissociation of ammonia on graphene oxides: A first-principles study. *J. Phys. Chem. C* **2012**, *116*, 8778–8791.
[67] Malvankar, N. S.; Vargas, M.; Nevin, K. P.; Franks, A. E.; Leang, C.; Kim, B. C.; Inoue, K.; Mester, T.; Covalla, S. F.; Johnson, J. P. et al. Tunable metallic-like conductivity in microbial nanowire networks. *Nat. Nanotechnol.* **2011**, *6*, 573–579.
[68] Lechner, B. A. J.; Kim, Y.; Feibelman, P. J.; Henkelman, G.; Kang, H.; Salmeron, M. Solvation and reaction of ammonia in molecularly thin water films. *J. Phys. Chem. C* **2015**, *119*, 23052–23058.
[69] Lim, D. W.; Sadakiyo, M.; Kitagawa, H. Proton transfer in hydrogen-bonded degenerate systems of water and ammonia in metal-organic frameworks. *Chem. Sci.* **2019**, *10*, 16–33.
[70] Ueki, T.; Walker, D. J. F.; Woodard, T. L.; Nevin, K. P.; Nonnenmann, S. S.; Lovley, D. R. An escherichia coli chassis for production of electrically conductive protein nanowires. *ACS Synth. Biol.* **2020**, *9*, 647–654.
[71] Yin, B.; Liu, X. M.; Gao, H. Y.; Fu, T. D.; Yao, J. Bioinspired and bristled microparticles for ultrasensitive pressure and strain sensors. *Nat. Commun.* **2018**, *9*, 5161.
[72] Ueki, T.; Walker, D. J. F.; Tremblay, P. L.; Nevin, K. P.; Ward, J. E.; Woodard, T. L.; Nonnenmann, S. S.; Lovley, D. R. Decorating microbially produced protein nanowires with peptide ligands. *ACS Synth. Biol.* **2019**, *8*, 1809–1817.